Available online at www.sciencedirect.com
ScienceDirect
Journal of Sound and Vibration 312 (2008) 576–583
JOURNAL OF SOUND AND VIBRATION
www.elsevier.com/locate/jsvi

On the impulse response precursor of an ideal linear hysteretic damper

Kui-Fu Chen[a,*], Sen-Wen Zhang[b]

[a]China Agricultural University, PB# 74, East Campus, Beijing 100083, PR China
[b]The Institute of Applied Mechanics, Jinan University, Guangzhou 510632, PR China

Received 11 April 2005; received in revised form 6 April 2006; accepted 11 July 2007
Available online 18 December 2007

Abstract

The model of the ideal linear hysteretic damper has been shown to possess a non-causal impulse response precursor. However, the relevant characteristics of the impulse response precursor (its extremum, monotonicity, and asymptotic property) were not well comprehended in the literature. In this paper, an impulse response precursor expression was derived. It was observed that the impulse response precursor achieves its only extremum, which is negative, at the origin. The impulse response precursor monotonically increases from this extremum to zero while time retraces to the negative infinity. The asymptotic rate of impulse response precursor approaching zero is $O(1/t)$. The non-causal size gets stronger as the loss factor increases. Numerical computation also shows that the non-causal extremum is even deeper than the first trough of the causal portion of the impulse response when the loss factor is greater than 0.77.

1. Introduction

A linear viscous damping model is theoretically the simplest. This model assumes that the energy loss per cycle of vibration is proportional to the vibration frequency. A more general damping model assumes that the energy loss per cycle varies with the vibration frequency [1]. Experiments have shown that its simplest form, a frequency-independent model, could cover the damping property of many materials. This frequency independent model, or "rate-independent" damping model, has alternative names such as linear hysteretic damping, structural damping, material damping, complex stiffness, and internal damping. In addition, Crandall introduced the concept of the band-limited hysteretic damper, so he called the conventional whole band rate-independent damper the ideal linear hysteretic damper [2].

While the rate-independent damping model looks simple in the frequency domain, it has an unusual characteristic in the time domain which has puzzled scientists for a long time. The characteristic in question is the non-causal response of the model to the impulse, i.e., the system reacts before the impulse is applied to the system. It is known as the impulse response precursor and has been confirmed [3–9] and stressed over and over [10–13].

*Corresponding author.
E-mail addresses: chenkuifu@gmail.com, chenkuifu@yahoo.com (K.-F. Chen).

0022-460X/$ - see front matter © 2007 Elsevier Ltd. All rights reserved.
doi:10.1016/j.jsv.2007.07.091

A real world physical system must be causal and stable. One philosophy, to avoid the non-causality, replaces the rate-independent damping model with a revised one. Makris had developed this kind of model [14], although the new model's stiffness was no longer a constant.

A second philosophy is to just ignore the impulse response precursor, which is achieved either implicitly or explicitly. For example, if the impulse response function is used explicitly, the impulse response precursor simply is designated as zero. Generally, the impulse response function is used implicitly in a frequency domain analysis, and it was shown that the contribution from non-causality is minor for a lightly damped system and can be neglected from a practical point of view [15]. In particular, for the lightly damped systems which frequently occur in engineer structural analysis, the differences in magnification factors between the rate-independent damping model and the equivalent viscous damping model are shown not to be significant [16]. Approximating the hysteretic damping matrix with a viscous matrix was studied systematically by Henwood [12].

Overtly, the hypothesis of the second philosophy is that the impulse response precursor must be small compared to the causal portion, and the impulse response precursor must attenuate to zero while time approaches the negative infinity. Crandall [17] showed that for a lightly damped system, via Taylor's expansion and elegant integral manipulation, this hypothesis is true in the first-order approximation. However, to the authors' knowledge, a systematic analysis was not available in literature.

Interestingly, several numerical simulations are consistent with this hypothesis that impulse response precursor attenuates to zero with time approaching the negative infinity. Nevertheless, the numerical approach is not always amenable, for example the results shown by Gaul et al. [3] conflicted with others. In Fig. 4 of their paper, the computational impulse response precursor with a loss factor 0.05 is not monotonic, and the minimum is not at the origin either.

In this paper, an impulse response precursor expression is derived, which is achieved by applying the residue theorem and the contour integration. This expression benefits the impulse response precursor sketch analysis. It was uncovered that the impulse response precursor does achieve only one extremum at the origin and does monotonically decrease with negative time. The impulse response precursor is negative and approaches zero at the rate $O(1/t)$. The non-causal degree aggravates as the loss factor increases. Moreover the numerical computation shows that the non-causal extremum is deeper than the first trough of the causal portion for a large loss factor.

2. Retrieving the impulse response precursor

The physical model of an ideal linear hysteretic damper originates from the vibrator damped by a frictional force (see Ref. [18] and references therein), which is nonlinear. The ideal linear hysteretic damper is a linear system with the frequency response function as follows:

$$H(\mathrm{j}\omega) = [m(\mathrm{j}\omega)^2 + k(1 + \mathrm{j}\eta \operatorname{sign}\omega)]^{-1}, \tag{1}$$

where m, k are system mass and stiffness, respectively, and $\eta > 0$ is the loss factor.

While Eq (1) looks simple in the frequency domain, its equivalent ordinary differential is not so straightforward, which has fascinated scientists working on this topic for a long time. The current consensus is this has been solved by using integro-differential equations [6,8,19–21]. For the ideal linear hysteretic damping, the integro-differential portion degenerates to the Hilbert transform, which was discovered by Inaudi and Kelly [6] and Chen and You [8]. This also indicates that the hysteretic damping model does possess a time-invariant system, but the system order is infinite.

Now we turn to the unitary impulse response function (UIRF) $h(t)$, which is the inverse Fourier transform of the frequency response function $H(\mathrm{j}\omega)$:

$$h(t) = \frac{1}{2\pi}\int_{-\infty}^{+\infty} H(\mathrm{j}\omega)\exp(\mathrm{j}\omega t)\,\mathrm{d}\omega. \tag{2}$$

The non-causality, i.e., $h(t)$ in Eq (2) is non-zero for $t \leqslant 0$, had been proved in literature. In Ref. [3], it is based on two facts. First, because $H(\mathrm{j}\omega) \propto (\mathrm{j}\omega)^{-2}$ as $|\omega| \to \infty$, $h(t)$ is continuous. Second, $h(0) \neq 0$. In light of

these two facts, and the property of a continuous function [22], there exists a neighboring interval around $t = 0$, over which $h(t)$ is not zero. The non-zero portion before $t = 0$ is the impulse response precursor.

In the ensuing impulse response precursor property study, we use contour integration and residue theory. First, the frequency response function needs to be extended into a transfer function. This is obtained via substituting $j\omega$ in Eq (1) with complex $s = j\omega+\sigma$. On the complex plane depicted in Fig. 1, the transfer function is

$$H(s) = m^{-1}\left(\omega_n^2 + s^2 + j\eta\omega_n^2 \mathrm{sign}[\mathrm{Im}(s)]\right)^{-1}, \tag{3}$$

where $\omega_n = \sqrt{k/m}$ is the circular natural frequency without damping.

Second, we need the transfer function poles, which are given by the roots of the denominator

$$\omega_n^2 + s^2 + j\eta\omega_n \mathrm{sign}[\mathrm{Im}(s)]\omega_n = 0. \tag{4}$$

Eq. (4) has two and only two roots as follows:

$$s_1 = (j\mu - \lambda)\omega_n, \quad s_2 = (-j\mu - \lambda)\omega_n, \tag{5}$$

where

$$\mu = \sqrt{(\sqrt{1+\eta^2}+1)/2}, \quad \lambda = \sqrt{(\sqrt{1+\eta^2}-1)/2}. \tag{6}$$

It must be stressed that the system has only the above two poles, not four poles as claimed in some literature. These two poles are symmetrical to the imaginary axis and both are stable. Nonetheless, the stability of the whole system is equivocal [13].

When we consider the precursor, which is defined over the negative time, the integral contours are chosen on the upper half complex plane. This is depicted in Fig. 1, $C_\omega \to C_R \to C_\delta$ and $C_{-\omega} \to C_{-R} \to C_{-\delta}$. The reason of choosing C_δ and $C_{-\delta}$ is because $H(s)$ is not analytical along $\mathrm{Re}(s) = 0$.

Now consider the right contour $C_\omega \to C_R \to C_\delta$. Since it lies in the analytical domain and does not encircle any pole, in light of the residue theorem, the following equation holds:

$$\int_{C_\omega} H(s)\exp(st)\,ds + \int_{C_R} H(s)\exp(st)\,ds + \int_{C_\delta} H(s)\exp(st)\,ds = 0. \tag{7}$$

On the upper half-complex plane, the second term will vanish as the radius R of the arch C_R approaches infinity. This is because the integrand $|H(s)\exp(st)| \leqslant |H(s)| = O(R^{-2})$ as $R \to \infty$.

Now while $\delta \to 0$ and $R \to \infty$, the first term and third term become as

$$\int_{C_\omega} H(s)\exp(st)\,ds = j\int_{0^+}^{\infty} H(j\omega)\exp(j\omega t)\,d\omega, \tag{8}$$

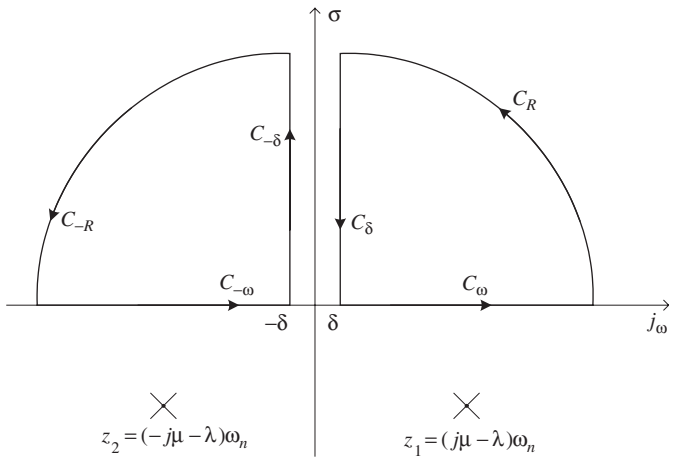

Fig. 1. Sketch of integration contour.

$$\int_{C_\delta} H(s)\exp(st)\,\mathrm{d}s = \int_{\infty}^{0} H(\sigma + \mathrm{j}0^+)\exp(\sigma t)\,\mathrm{d}\sigma. \tag{9}$$

Note that the low integral bound in Eq. (8) is 0^+, which excludes 0 intentionally, since $H(s)$ is not analytical at $s = 0$. In light of above argument, we have

$$\mathrm{j}\int_{0^+}^{\infty} H(\mathrm{j}\omega)\exp(\mathrm{j}\omega t)\,\mathrm{d}\omega + \int_{\infty}^{0} H(\sigma + \mathrm{j}0^+)\exp(\sigma t)\,\mathrm{d}\sigma = 0. \tag{10}$$

For the left contour $C_\omega \to C_R \to C_\delta$, in the same vein, we have

$$\mathrm{j}\int_{\infty}^{0^-} H(\mathrm{j}\omega)\exp(\mathrm{j}\omega t)\,\mathrm{d}\omega + \int_{0}^{\infty} H(\sigma + \mathrm{j}0^-)\exp(\sigma t)\,\mathrm{d}\sigma = 0. \tag{11}$$

Adding Eqs. (11) and (12), we have

$$\mathrm{j}\left[\int_{0^+}^{\infty} H(\mathrm{j}\omega)\exp(\mathrm{j}\omega t)\,\mathrm{d}\omega + \int_{\infty}^{0^-} H(\mathrm{j}\omega)\exp(\mathrm{j}\omega t)\,\mathrm{d}\omega\right] - \int_{0}^{\infty} [H(\sigma + \mathrm{j}0^+) - H(\sigma + \mathrm{j}0^-)]\exp(\sigma t)\,\mathrm{d}\sigma = 0. \tag{12}$$

The integral contour of Eq. (2) is along the imaginary axis from negative infinity to positive infinity. Since $H(\mathrm{j}\omega)$ owns the first class discontinuity at $\omega = 0$, we have $\int_{0^-}^{0^+} H(\mathrm{j}\omega)\exp(\mathrm{j}\omega t)\,\mathrm{d}\omega = 0$. This means that the result of the first square bracket is nothing but $2\pi h(t)$. Thus

$$h(t) = \frac{1}{2\pi\mathrm{j}}\int_{0}^{\infty} [H(\sigma + \mathrm{j}0^+) - H(\sigma + \mathrm{j}0^-)]\exp(\sigma t)\,\mathrm{d}\sigma. \tag{13}$$

Substituting Eq. (3) into Eq. (13) yields

$$h(t) = -\frac{\eta}{\pi m\omega_n} I(t), \tag{14}$$

where

$$I(t) = \omega_n^3 \int_0^{\infty} \frac{\exp(\sigma t)}{(\omega_n^2 + \sigma^2)^2 + \eta^2\omega_n^4}\,\mathrm{d}\sigma = \int_0^{\infty} \frac{\exp(\sigma\omega_n t)}{(1 + \sigma^2)^2 + \eta^2}\,\mathrm{d}\sigma. \tag{15}$$

The above discussion is for $t < 0$. The causal part for $t \geqslant 0$ has been obtained in Ref. [3]. Combining these together yields

$$m\omega_n h(t) = \begin{cases} -\dfrac{\eta}{\pi} I(t), & t < 0, \\ \dfrac{\exp(-\lambda\omega_n t)}{\mu^2 + \lambda^2}[\mu\sin(\mu\omega_n t) - \lambda\cos(\mu\omega_n t)] + \dfrac{\eta}{\pi} I(-t), & t \geqslant 0, \end{cases} \tag{16}$$

Bonisoli and Mottershead [23] had given similar argument in lieu of complex-damped system.

2.1. Remarks

Generally, the causality of a model with complex forms of damping is not always easy to decide. The above argument infers a corollary for determining the causality of a stable system. That is, if a stable system satisfies that: (1) its transfer function is analytical on the upper half-complex plane; (2) $H(s)$'s attenuating rate is greater than $|s|^{-1}$ while $|s| \to \infty$, then this system is causal.

In addition, if the transfer function of a stable system is not analytical in the upper half-plane, the non-analytic nature is very likely a first class discontinuity, since a stable system cannot have any poles on the upper half-plane. If the contour integral is employed to study the causality, the contour segments had better be allocated parallel to the two sides of the discontinuity.

3. Impulse response precursor properties

In light of Eq. (14), we can immediately conclude that the impulse response precursor achieves the minimum at $t = 0$, which is also the only one impulse response precursor extremum. Naturally, this extremum indicates the non-causal size. Its exact value had been given as follows [3,17]:

$$m\omega_n h(0) = -\frac{\lambda}{2(\lambda^2+\mu^2)} = -\sqrt{\frac{\sqrt{1+\eta^2}-1}{8(1+\eta^2)}}. \tag{17}$$

In Fig. 2 it is shown that the size of this impulse response precursor extremum monotonically increases with η. For a large η, $h(0)$ is significantly different from zero, for example, $m\omega_n h(0) \approx -0.1609$ for $\eta = 1$. The dash line depicts $-\eta/4$, which is a good approximation when η^2 is small [3].

For a specified η, Eq. (14) also shows that the impulse response precursor monotonically decreases as time develops, and is always negative. Towards the negative time direction, the impulse response precursor approaches zero at the rate $O(t^{-1})$. This can be argued as follows:

$$I(t) = \int_0^\infty \frac{\exp(\sigma\omega_n t)}{(1+\sigma^2)^2+\eta^2}\,\mathrm{d}\sigma \leqslant \int_0^\infty \exp(\sigma\omega_n t)\,\mathrm{d}\sigma = \frac{1}{\omega_n t}. \tag{18}$$

Both the non-causal portion and causal portion use $I(t)$, but it is difficult to work out a closed-form $I(t)$, if not impossible. Therefore, we have to make use of a numerical approach. The upper integral bound of $I(t)$ is infinite, but both $\exp(\sigma\omega_n t)$ and $[(1+\sigma^2)^2+\eta^2]^{-1}$ attenuates to zero as σ approaches infinity. Hence, the infinite bound can be truncated to be a finite bound provided that the finite bound is large enough. For a given finite bound b, $I(t)$ is more infectious at a time close to the origin.

To inhibit the error due to truncating the infinite bound, the contribution outside the interval $[0,b]$ can be approximately modeled by some tricks. For a large b, $[(1+\sigma^2)^2+\eta^2]^{-1}$over $[b,\infty]$ can be approximated as σ^{-4}, so

$$\int_b^\infty \frac{\exp(\sigma\omega_n t)}{(1+\sigma^2)^2+\eta^2}\,\mathrm{d}\sigma \approx \int_b^\infty \frac{\exp(\sigma\omega_n t)}{\sigma^4}\,\mathrm{d}\sigma = \frac{1}{b^3}E_4(-b\omega_n t). \tag{19}$$

Here $E_k(x)$ is the exponential integral as

$$E_k(x) = \int_1^\infty \frac{\exp(-x\sigma)}{\sigma^k}\,\mathrm{d}\sigma. \tag{20}$$

In brief, $I(t)$ can be approximated as

$$I(t) \approx \int_0^b \frac{\exp(\sigma\omega_n t)}{(1+\sigma^2)^2+4\eta^2}\,\mathrm{d}\sigma + \frac{1}{b^3}E_4(-b\omega_n t). \tag{21}$$

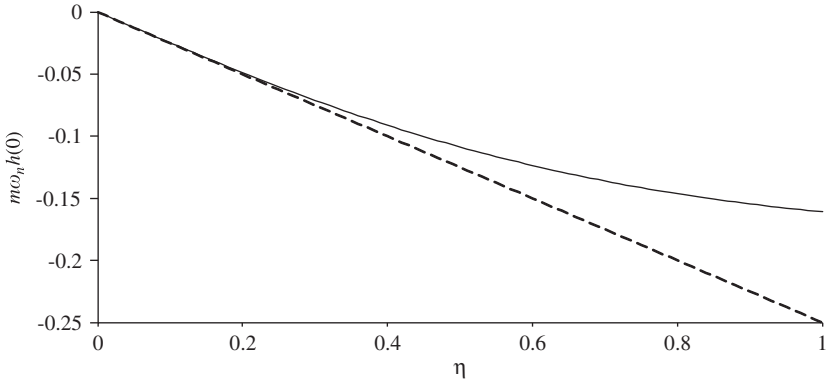

Fig. 2. Non-causal degree depending on the loss factor. Here the solid line stands for $m\omega_n h(0) = -\sqrt{(\sqrt{1+\eta^2}-1)/8(1+\eta^2)}$, and the dash line stands for $-\eta/4$.

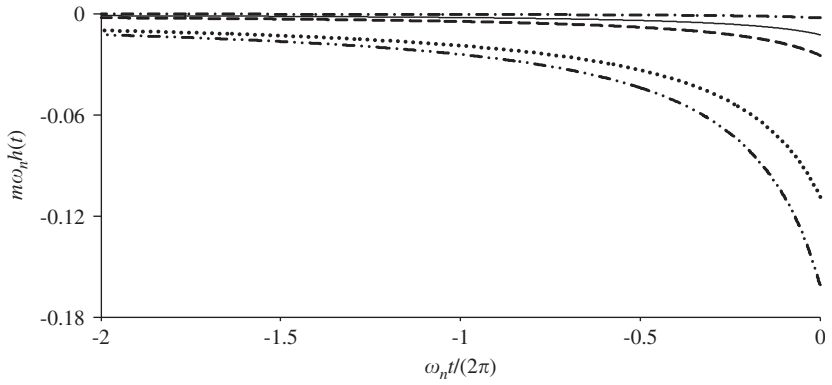

Fig. 3. Impulse response precursors for five loss factors. Here, symbols stand for (– · – · –) $\eta = 0.01$; (——) $\eta = 0.05$; (– – –) $\eta = 0.1$; (… …) $\eta = 0.5$; and (– · · –) $\eta = 1$. The computational parameters are $b = 10$ and $\Delta b = 0.01$.

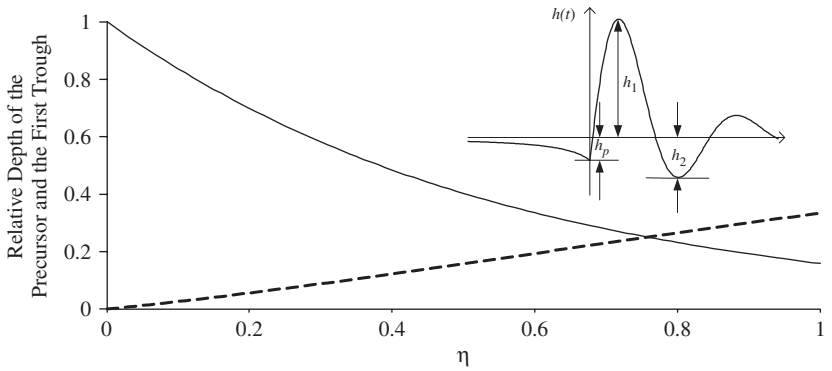

Fig. 4. Size comparison among the impulse response precursor, the first causal peak, and the first trough. Here, the solid line and dash line stand for h_2/h_1 and h_p/h_1, respectively.

The first term can be obtained by a normal numerical integration. Computing the second term, the exponential integral, is discussed in detail in Ref. [24].

Shown in Fig. 3 are computational results for five typical cases of η. The numerical integration for the first term is the Simpson's rule with the computational parameters listed in the figure. For the employed parameter, $b = 10$, the contribution of the second term of Eq. (21) is very small.

The computed impulse response precursors are consistent with the aforementioned qualitative properties: being negative, achieving the extremum at time zero, and monotonically approaching zero as time progresses towards minus infinity.

To delineate the non-causal degree, the ratio of the non-causal extremum to the highest peak of the causal portion is plotted in Fig. 4. The causal portion is computed from Eq (17), and the computational parameter and algorithm are the same as those used to generate data (Fig. 3).

As the loss factor η increases, the precursor size h_p increases monotonically (also see Fig. 4), and the first peak h_1 decreases monotonically. These two trends lead that the ratio h_p/h_1 increases almost linearly, and h_p/h_1 can be as high as around 1/3 for $\eta = 1$. Also shown is h_2/h_1, the ratio of the first trough depth to the first peak h_1. h_2/h_1 decreases monotonically as η. When $\eta \approx 0.77$, h_2/h_1 is about the same as h_p/h_1. When η is transgresses over this point, the non-causal precursor is even deeper than the first trough.

These features demonstrate that for a larger loss factor, the non-causal portion is significant, and cannot be ignored. A viscous substitution is not defendable for this case.

It was argued that $\dot{h}(0^+) = (3\pi + 2\tan\eta^{-1})/(4m\pi)$, but for a causal system $\dot{h}(0^+) = m^{-1}$, which infers that the unitary pulse is transferred to the system, and the system obtains velocity as m^{-1}. However, for the ideal

hysteretic damper, it is easy to verify that $\dot{h}(0^+) - \dot{h}(0^-) = m^{-1}$, which implies that the unitary pulse changes the system velocity by m^{-1}.

4. Summary

The ideal linear hysteretic damper possesses a non-causal impulse response precursor, which was proved theoretically and confirmed numerically. For most numerical simulations, impulse response precursor achieves minimum at time zero, and approaches zero monotonically when time approaches negative infinity. A hypothesis for ignoring the non-causal portion necessitates that these properties had to be proved theoretically.

In this paper, an impulse response precursor expression was derived in light of the residue theorem. Based on this expression, it can be argued theoretically that the impulse response precursor achieves the extremum at time zero, and its size monotonically decreases towards zero and the negative time direction. The impulse response precursor is negative and approaches zero by the rate $O(1/t)$. The non-causal size becomes larger as the loss factor increases. Numerical computation was used to show that the non-causal extremum is deeper than the first trough of the causal portion when the loss factor is greater than 0.77.

Acknowledgments

Our thanks to Mr. Stephen Crowsen, David Leon and Erik Koht for their assistance with editing this paper.

References

[1] S.H. Crandall, The role of damping in vibration theory, *Journal of Sound and Vibration* 11 (1970) 3–18.
[2] S.H. Crandall, Hysteretic damping model in vibration theory, *Proceedings of the Institution of Mechanical Engineers, Part C: Mechanical Engineering Science* 205 (1991) 23–28.
[3] L. Gaul, S. Bohlen, S. Kempfle, Transient and forced oscillations of systems with constant hysteretic damping, *Mechanics Research Communications* 12 (1985) 187–201.
[4] H.K. Milne, The impulse response function of a single degree of freedom system with hysteretic damping, *Journal of Sound and Vibration* 100 (1985) 590–593.
[5] D.I.G. Jones, Impulse response function of a damped single degree of freedom system, *Journal of Sound and Vibration* 106 (1986) 353–356.
[6] J.A. Inaudi, J.M. Kelly, Linear hysteretic damping and the Hilbert transform, *Journal of Engineering Mechanics-ASCE* 121 (1995) 626–632.
[7] B.F.J. Spencer, L.A. Bergman, Stochastic response of systems with linear hysteretic damping, *Proceedings of the 11th Conference on Engineering Mechanics*, Fort Lauderdale, FL, 1996, pp. 677–680.
[8] J.T. Chen, D.W. You, Integral–differential equation approach for the free vibration of a SDOF system with hysteretic damping, *Advances in Engineering Software* 30 (1999) 43–48.
[9] H. Tsai, T. Lee, Dynamic analysis of linear and bilinear oscillators with rate-independent damping, *Computers and Structures* 80 (2002) 155–164.
[10] S.H. Crandall, New hysteretic damping model?, *Mechanics Research Communications* 22 (1995) 201.
[11] S.H. Crandall, Ideal hysteretic damping is noncausal, *Zeitschrift fuer Angewandte Mathematik und Mechanik, ZAMM (Applied Mathematics and Mechanics)* 77 (1997) 711.
[12] D.J. Henwood, Approximating the hysteretic damping matrix by a viscous matrix for modelling in the time domain, *Journal of Sound and Vibration* 254 (2002) 575–593.
[13] P.D. Spanos, B.A. Zeldin, Pitfalls of deterministic and random analyses of systems with hysteresis, *Journal of Engineering Mechanics-ASCE* 126 (2000) 1108–1110.
[14] N. Makris, Causal hysteretic element, *Journal of engineering mechanics-ASCE* 123 (1997) 1209–1214.
[15] J.P. Wolf, G.R. Darbre, Time-domain boundary element method in viscoelasticity with application to a spherical cavity, *Soil Dynamics and Earthquake Engineering* 5 (1986) 138–148.
[16] A.K. Chopra, Damping in structures, in: *Dynamics of Structures: Theory and Applications to Earthquake Engineering*, Prentice-Hall, Englewood Cliffs, NJ, 2000, pp. 409–428.
[17] S.H. Crandall, Dynamic response of systems with structural damping, in: S. Lees (Ed.), *Air, Space and Instruments, Draper Anniversary*, McGraw-Hill, New York, 1963, pp. 183–193.
[18] G.B. Muravskii, On frequency independent damping, *Journal of Sound and Vibration* 274 (2004) 653–668.
[19] J.A. Inaudi, N. Makris, Time-domain analysis of linear hysteretic damping, *Earthquake Engineering and Structural Dynamics* 25 (1996) 529–545.

[20] N.M.M. Maia, J.M.M. Silva, A.M.R. Ribeiro, On a general model for damping, *Journal of Sound and Vibration* 218 (1998) 749–767.
[21] S. Adhikari, Dynamics of nonviscously damped linear systems, *Journal of Engineering Mechanics-ASCE* 128 (2002) 328–339.
[22] C.K. Chui, *An Introduction to Wavelets*, Academic Press, Boston, USA, 1992, pp. 23–26.
[23] E. Bonisoli, J.E. Mottershead, Complex-damped dynamic systems in the time and frequency domains, *Shock and Vibration* 11 (2004) 209–225.
[24] W.H. William, S.A. Teukolsky, W.T. Vetterling, *Numerical Recipes in C—The Art of Scientific Computing*, Cambridge University Press, Cambridge, UK, 1998, pp. 222–226.